The dentin–enamel junction and the fracture of human teeth

V. IMBENI[1]*, J. J. KRUZIC[1], G. W. MARSHALL[2], S. J. MARSHALL[2] AND R. O. RITCHIE[1]#

[1]Materials Sciences Division, Lawrence Berkeley National Laboratory, and Department of Materials Science and Engineering, University of California, Berkeley, California 94720, USA
[2]Department of Preventive and Restorative Dental Sciences, University of California, San Francisco, California 94143, USA
*Present address: SRI International, Menlo Park, California 94025, USA
#e-mail: RORitchie@lbl.gov

Published online: 13 February 2005; doi:10.1038/nmat1323

The dentin–enamel junction (DEJ), which is the interfacial region between the dentin and outer enamel coating in teeth, is known for its unique biomechanical properties that provide a crack-arrest barrier for flaws formed in the brittle enamel[1]. In this work, we re-examine how cracks propagate in the proximity of the DEJ, and specifically quantify, using interfacial fracture mechanics, the fracture toughness of the DEJ region. Careful observation of crack penetration through the interface and the new estimate of the DEJ toughness (~5 to 10 times higher than enamel but ~75% lower than dentin) shed new light on the mechanism of crack arrest. We conclude that the critical role of this region, in preventing cracks formed in enamel from traversing the interface and causing catastrophic tooth fractures, is not associated with the crack-arrest capabilities of the interface itself; rather, cracks tend to penetrate the (optical) DEJ and arrest when they enter the tougher mantle dentin adjacent to the interface due to the development of crack-tip shielding from uncracked-ligament bridging.

The DEJ in teeth represents the zone between two distinct calcified tissues with very different biomechanical properties: enamel and dentin[1]. Enamel is the hard and brittle outer portion of the tooth that envelops the softer dentin; it comprises defective carbonate-rich apatite crystals arranged in enamel rods (4–5 μm in diameter) or prisms that lie nearly perpendicular to the DEJ[2,3]. Its fracture toughness (K_c) typically ranges from ~0.7 MPa m$^{1/2}$ in the direction parallel to the enamel rods to ~1.3 MPa m$^{1/2}$ in the perpendicular direction[4,5]. Dentin, conversely, is a biological composite that is tougher than enamel and similar at the nanostructural level to bone. It has a unique architecture consisting of dentinal tubules, ~1 μm in diameter, surrounded by peritubular dentin, consisting of ~0.5–1-μm-thick cylinders of randomly oriented apatite crystallites. These tubular units are embedded in a collagen matrix–apatite reinforced composite. As the tubules are the formative tracks of the odontoblastic cells that move inward and reside on the pulp chamber surface, there are substantial variations in morphology and structure of the dentin from the DEJ to the pulp chamber[6]. Dentin has a K_c toughness that varies between 1.0 and 2.0 MPa m$^{1/2}$ in directions perpendicular and parallel to the tubules[7,8]. The toughness of dentin adjacent to the DEJ, so-called mantle dentin, is supposedly higher due

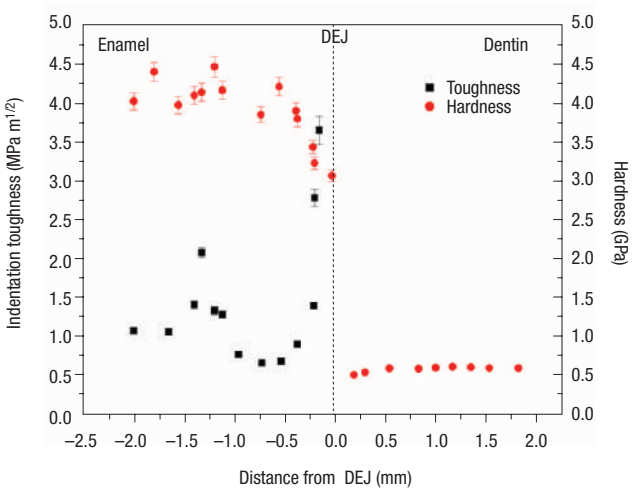

Figure 1 Typical profiles of the Vickers hardness and the indentation toughness. Profiles taken normal to, and across, the DEJ region from the enamel to the dentin in a human molar. Hardness indentations were made with a load range between 3 and 5 N to minimize brittle fracture damage, but to still form cracks around the indents to enable toughness measurements. Lines of indents were performed on three different teeth (each from a unique patient), with three series for each tooth. The indentation toughness[28], $K_{ind,c}$, was determined from the indentation load P, and the average crack lengths, c, emanating from the indent corners, according to $K_{ind,c} = \chi P/c^{3/2}$, where χ is the residual indentation coefficient (taken as 0.076 for enamel[4]). Such measurements could only be made in the enamel as inelasticity in the dentin suppresses the formation of indent cracks. These profiles show that cracks in the enamel experience a region of decreasing hardness yet increasing toughness as they approach the DEJ. Error bars on all data points are based on the resolution of the optical microscope, that is, on the uncertainty in measuring the size of the indents and indent cracks.

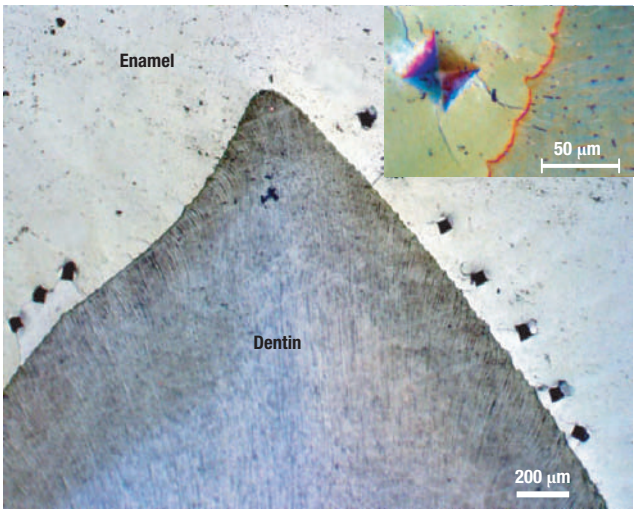

Figure 2 Optical micrograph of the placement of Vickers indents in the enamel. The indents were within ~20–50 μm from the optical DEJ in a human molar, which were used to create cracks that impact upon the DEJ. Inset shows optical micrograph with Nomaski interference contrast of one such indentation with cracks, which emanate from the indent corners, propagating into the scalloped interface.

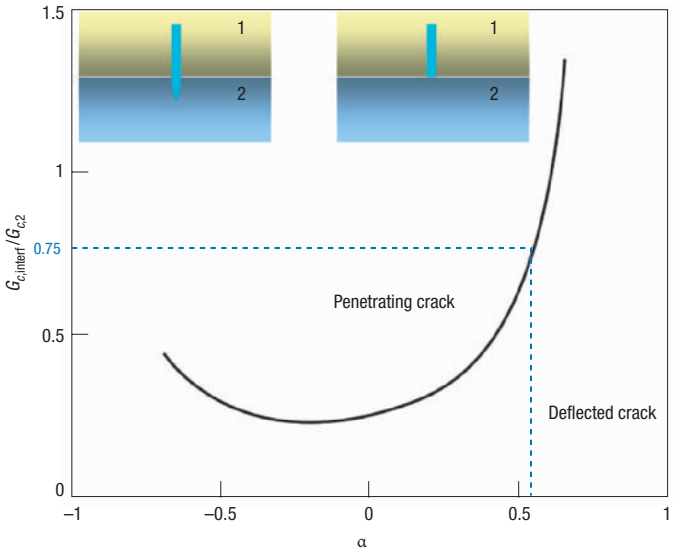

Figure 3 The linear-elastic solutions of He and Hutchinson[22]. Determination of the conditions for a normally incident crack to penetrate or deflect along an interface between two materials 1 and 2. Whether the crack penetrates or not is a function of the (i) impingement angle, (ii) the elastic mismatch across the interface, defined by the first Dundurs' parameter α (ref. 29; for definition, see text), and (iii) relative magnitude of the interface toughness and the toughness of material 2 (dentin) on the far side of the interface, ($G_{c,interf}/G_{c2}$). The figure shows a plot of $G_{c,interf}/G_{c2}$ as a function of the modulus mismatch α. For the enamel/dentin junction where $\alpha \sim 0.53$, the absence of interface delamination leads to a criticality between penetration and arrest at the DEJ, which can be used to estimate a lower-bound for the toughness of the DEJ region, $G_{c,interf}$, given by 0.75 of $G_{c,interf}/G_{c2}$. Note that these solutions represent a two-dimensional description of crack paths in isotropic materials; their use here for dentin and enamel, which are anisotropic, is considered acceptable as the analysis is performed principally on normally-incident cracks.

to its lower mineral content and reduced modulus[9]; the tubules in this region are comparatively rare or absent.

The DEJ itself has a hierarchical microstructure with a three-dimensional scalloped appearance along the interface[1]. It is an anatomically thin region with a broader functional width; it represents a functionally graded zone where the enamel and dentin close to the interface have slightly different microstructures and properties than the more distant bulk phases. Specifically, the morphology of the collagen is such that type-I fibrils emanate from the dentin and project fibrils (~100 nm in diameter) perpendicular to the DEJ[10]; such Von Korf's fibres cross the DEJ and appear to be inserted directly into the enamel. In contrast, collagen fibrils in bulk dentin are either parallel or at angles less than 90° to the plane of the junction[1].

Although the fracture-resistant properties of the DEJ are believed to originate from a gradual change in microstructure and properties of dentin and enamel rather than from an abrupt transition between two dissimilar materials[11,12], the DEJ appears as a 'line' when imaged microscopically. This apparently sharp interface, the 'optical DEJ', is thought to represent the original position of the basement membrane of the ameloblasts and odontoblasts, where they contact in the embryological tooth bud. Often interfaces between materials with dissimilar elastic and mechanical properties are 'weak links' in a structure; the DEJ region, however, acts to successfully transfer applied loads (for example, masticatory or impact) from the enamel to the dentin and can inhibit cracks in enamel from propagating into the dentin and causing catastrophic fracture of the tooth[13]. Although there have been numerous attempts to explain this latter function[5,11,13–20], including that the DEJ is tougher than either dentin or enamel[1] because it is less mineralized[19] and contains more collagen[1,13], that it may reduce the stress concentration[1,20], or that it promotes crack deflection[14] due to microhardness[2,19] or modulus[11] differences across the interface, there is little consensus on the origin of the DEJ's crack-arrest properties.

There is also inconsistent information on the toughness of the DEJ region compared with that of enamel and dentin. Specifically, the DEJ toughness values reported differ by a factor of three or more—from 336 J m^{-2} (refs 15,16) to 988 J m^{-2} (ref. 13) when described in terms of a critical strain-energy release rate (G_c) and from 0.6–0.9 MPa m$^{1/2}$ (refs 2,6) to 3.4 MPa m$^{1/2}$ (ref. 13) when presented as a critical stress intensity (K_c); indeed, in our opinion there have been only a few realistic measurements[13,14]. Accordingly, in this work, we apply a novel technique involving propagating indentation cracks into the interfacial region in human teeth to assess quantitatively the toughness of the DEJ; further, we identify the microstructural mechanisms by which the DEJ region functions to inhibit cracks from traversing the interface to cause catastrophic tooth fracture.

To assess the variation in properties across the interface, we measured Vickers hardness and indentation toughness profiles under hydrated conditions normal to the DEJ (Fig. 1). Similar to previous results[11,13,16,18,20], this indicated that the hardness of the enamel falls quite rapidly within a millimetre of the optical DEJ to reach a minimum in the mantle dentin in close proximity to the interface. Corresponding indentation toughness measurements show that the toughness of the enamel also has a minimum close to the optical DEJ, but then rises steeply over the final ~500 μm into the interface. These profiles clearly indicate that mechanical properties vary over a region of several hundred micrometres across the interface, but that cracks in the enamel experience a region of decreasing hardness yet increasing toughness as they impact the optical DEJ.

To evaluate quantitatively the toughness of the DEJ, we placed a series of Vickers microhardness indents (~40–50 per tooth) in polished sections of 13 non-carious extracted human molars

(11 axial and two occlusal sections), each tooth being unique to a single patient. Indents were made under hydrated conditions at ~20–50 μm from the optical DEJ on the enamel side (Fig. 2) such that cracks emanating from the corners of the indents would propagate towards the dentin and impinge onto the DEJ at differing angles of incidence. We then observed whether the cracks penetrated the interface, arrested or deflected along the optical DEJ. Knowing the modulus and toughness of the two phases on either side of the interface, we deduced the interface toughness using an 'interface impingement' technique developed for ceramics[21]. The basis of this method is the linear-elastic solutions of He and Hutchinson[22], which govern whether a crack, incident on a bimaterial interface, will deflect along, or penetrate through, the interface; this event depends specifically on (i) the angle of incidence, (ii) the elastic mismatch across the interface (which is a function of the relative elastic moduli), and (iii) the ratio of fracture toughnesses of the interface and the material on the far side of the interface ($G_{c,interf}/G_{c2}$) towards which the crack is propagating (Fig. 3).

Based on a total of 172 indentation cracks examined, we found that more than 75% of the cracks actually penetrated the optical DEJ a short distance, only to arrest after propagating ~10 μm or less into the mantle dentin. As the absolute resolution of the optical metallograph (×2,000) used to make this assessment was ~500 nm, there was some degree of uncertainty about the remaining cracks, which either arrested at the interface or penetrated it by less than ~500 nm. No evidence was seen of substantial interfacial delamination along the optical DEJ (except on dehydration in the conventional scanning electron microscope (SEM)). In general, most of these cracks were normally incident, as cracking in the enamel occurs by separation of the enamel rods and these are aligned roughly perpendicular to the DEJ. A few cracks that impinged on the optical DEJ at angles between ~30 and 75 degrees to the interface were found to penetrate.

Such observations were confirmed by imaging in the SEM (Fig. 4). It is apparent that once a crack penetrates the optical DEJ and comes to arrest in the mantle dentin, it is significantly bridged close to the crack tip by 'uncracked ligaments'. No such bridging was detected for cracking in enamel. The uncracked ligaments are regions of unbroken material, a few micrometres in dimension, that span the crack in the wake of the crack tip. In general, they are created either by the non-uniform advance of the crack front and/or by the imperfect linking of microcracks, initiated ahead of the crack tip, with the main crack[23]; in dentin, it is believed that they are created primarily by the latter process involving microcrack formation at the tubules ahead of the main crack[24]. The resulting uncracked-ligament bridging is a widely observed toughening mechanism in structural materials[23] and has been identified as one of the prominent contributions to the toughness of dentin[24] (and cortical bone[25]). The bridging mechanism acts to reduce the crack-driving force by sustaining a portion of the applied load that would otherwise contribute to cracking. In the present case, it is this reduction in crack-driving force due to such bridging that is responsible for bringing the crack to a halt, once it traverses the optical DEJ and encounters the higher collagen content of the dentin.

Crack bridging may also be responsible for the lack of incidence of cracks causing delamination along the optical DEJ. In samples where the interface cracked open under vacuum in the conventional SEM, clear evidence was seen of bridging by intact individual collagen fibrils that span the DEJ; indeed, such a mechanism of collagen-fibril bridging has been proposed for the toughening of bone[26]. This notion is consistent with the fact that the DEJ region is a complex interdigitation of enamel and dentin, with the enamel side being highly mineralized and the mantle dentin having more collagen, fewer tubules and less overall mineral than the bulk dentin. We thus believe that collagen fibrils perpendicular to the interface constitute the key

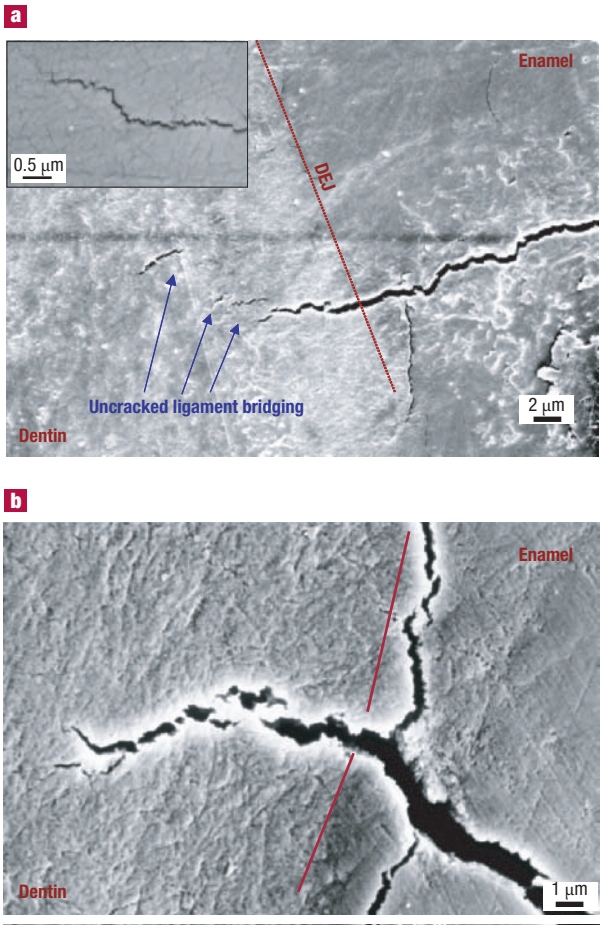

Figure 4 SEM examples of arrested cracks. Shown are cracks from the enamel that are normally incident on the optical DEJ and are arrested after propagating less than ~10 μm beyond the interface into the mantle dentin. Behind the arrested crack tip, numerous uncracked-ligament 'bridges' can be seen; these are regions of uncracked material that oppose the opening of the crack and sustain load that would otherwise be used for crack growth. Such bridging, which is a form of crack-tip shielding[30] and is a prominent toughening mechanism in dentin and bone[24,25], acts to reduce the effective driving force for crack extension, thereby arresting the crack. Inset shows the lack of such bridging for cracks in the enamel. Cracking can also be seen near, and nominally parallel, to the optical DEJ. However, by comparing these images with corresponding images in the environmental SEM (at ~1 kPa water pressure), such 'delamination' cracking was found to be an artefact caused by dehydration *in vacuo* in the conventional SEM.

reinforcing mechanism at the optical DEJ, which explains why so few cracking events cause delamination when they enter the DEJ region.

For cracks initiated in the enamel, this study shows that such cracks are stopped after penetrating the optical DEJ to arrest within ~10 μm into the mantle dentin, an event promoted by the generation of uncracked-ligament bridging. To quantify this, we note that the lack of evidence of interfacial delamination leads to a criticality between penetration and arrest at the interface, which can be used to estimate a lower-bound toughness of the DEJ region.

Considering a crack in the enamel (material 1) propagating into the dentin (material 2) and knowing the toughness of dentin, G_{c2}, and the elastic mismatch at the interface, characterized by the so-called 'Dundurs' parameter $\alpha = (E_1 - E_2) / (E_1 + E_2)$, where E_1 and E_2 are the respective Young's moduli of the enamel and

dentin, the toughness of the DEJ, $G_{c,interf}$, can be estimated from the He–Hutchinson solutions[22] for cracks perpendicular to an interface, specifically the $G_{c,interf}/G_{c2}$ versus α plot shown in Fig. 3. As these solutions are based on the strain-energy release rates rather than stress intensities, the value of the fracture toughness of dentin was calculated as $G_{c2} \sim 154$ J m^{-2} from the measured K_c value of 1.8 MPa m$^{1/2}$ determined in ref. 7. The modulus mismatch for the enamel–dentin interface is $\alpha \sim 0.53$, based on respective values[11] for the Young's moduli of enamel and dentin of 63.6 and 19.7 GPa. From Fig. 3, the critical ratio of the interface and matrix toughness, $G_{c,interf}/G_{c2}$, for penetration rather than interface arrest of normally incident cracks is ~0.75. This yields a lower-bound toughness of the DEJ of $G_{c,interf} \sim 115$ J m^{-2}, implying an actual toughness that is much higher than that of enamel ($G_{c1} \sim 10$–25 J m^{-2}) but only ~75% of that of dentin ($G_{c2} \sim 154$ J m^{-2}).

METHODS

MATERIALS

Thirteen sections of non-carious extracted human molars sterilized by gamma radiation were used in this study. Storage of samples until preparation was at 4 °C in distilled water with thymol. Sections were cut using a modified water-cooled diamond saw and the samples polished with 0.25-μm diamond paste. All samples were stored fully hydrated in Hanks' balanced salt solution (HBSS) before testing to prevent surface demineralization[27]; samples were additionally kept moist during testing by frequently spraying with HBSS.

CHARACTERIZATION

Crack trajectories were examined using optical, high-resolution and environmental SEM. Some sections were etched with H_3PO_4 (35% vol) to reveal microstructural features. Although samples were kept moist at all times, during imaging with conventional SEM (Topcon ICI DS130C), dehydration due to the vacuum sometimes led to cracking either along the line of indents or at/near the optical DEJ. To confirm that such spurious cracking did not compromise the results, samples were also examined in the environmental SEM (Hitachi, ESEM S-4300 SE/N) under a water vapour pressure of 1 kPa. Vickers hardness and indentation toughness tests were performed on a microhardness tester (Micromet, Buehler). The size of the indent and the indent cracks were determined with an Olympus STM-UMS optical microscope.

Received 8 September 2004; accepted 9 December 2004; published 13 February 2005.

References

1. Lin, C. P., Douglas, W. H. & Erlandsen, S. L. Scanning electron microscopy of Type I collagen at the dentin enamel junction of human teeth. *J. Histochem. Cytochem.* **41,** 381–388 (1993).
2. White, S. N. *et al.* The dentino-enamel junction is a broad transitional zone uniting dissimilar bioceramic composites. *J. Am. Ceram. Soc.* **83,** 238–240 (2000).
3. Ten Cate, A. R. *Oral Histology: Development, Structure, and Function* 4th edn (Mosby, St. Louis, Missouri, 1994).
4. Hassan, R., Caputo, A. A. & Bunshah, R. F. Fracture toughness of human enamel. *J. Dent. Res.* **40,** 820–827 (1981).
5. Xu, H. H. *et al.* Indentation damage and mechanical properties of human enamel and dentin. *J. Dent. Res.* **77,** 472–480 (1998).
6. Marshall, G. W., Marshall, S. J., Kinney, J. H. & Balooch, M. The dentin substrate: Structure and properties related to bonding. *J. Dent.* **25,** 441–458 (1997).
7. Imbeni, V., Nalla, R. K., Bosi, C., Kinney, J. H. & Ritchie, R. O. On the in vitro fracture toughness of human dentin. *J. Biomed. Mater. Res. A* **66,** 1–9 (2003).
8. Iwamoto, N. & Ruse, N. D. Fracture toughness of human dentin. *J. Biomed. Mater. Res. A* **66,** 507–512 (2003).
9. Tesch, W. *et al.* Graded microstructure and mechanical properties of human crown dentin. *Calcified Tissue Int.* **69,** 147–157 (2001).
10. Habelitz, S., Balooch, M., Marshall, S. J., Balooch, G. & Marshall, G. W. In situ atomic force microscopy of partially demineralized human dentin collagen fibrils. *J. Struct. Biol.* **38,** 227–236 (2002).
11. Marshall, G. W., Balooch, M., Gallagher, R. R., Gansky, S. A. & Marshall, S. J. Mechanical properties of the dentin-enamel junction: AFM studies of nanohardness, elastic modulus and fracture. *J. Biomed. Mater. Res.* **54,** 87–95 (2001).
12. Habelitz, S., Marshall, S. J., Marshall, G. W. & Balooch, M. The functional width of the dentino-enamel junction determined by AFM-based nanoscratching. *J. Struct. Biol.* **135,** 244–301 (2001).
13. Lin, C. P. & Douglas, W. H. Structure-property relations and crack resistance at the bovine dentin-enamel junction. *J. Dent. Res.* **73,** 1072–1078 (1994).
14. Dong, X. D. & Ruse, N. D. Fatigue crack propagation path across the dentinoenamel junction complex in human teeth. *J. Biomed. Mater. Res. A* **66,** 103–109 (2003).
15. Rasmussen, S. T. & Patchin, R. E. Fracture properties of human enamel and dentin in an aqueous environment. *J. Dent. Res.* **63,** 1362–1368 (1984).
16. Rasmussen, S. T. Fracture properties of human teeth in proximity to the dentinoenamel junction. *J. Dent. Res.* **63,** 1279–1283 (1984).
17. Lin, C. P. & Douglas, W. H. Fracture mechanics at the human dentin-resin interface: a fracture mechanics approach. *J. Biomech.* **27,** 1037–1047 (1994).
18. Urabe, I., Nakajima, M., Sano, H. & Tagami, J. Physical properties of the dentin-enamel junction region. *Am. J. Dent.* **13,** 129–135 (2000).
19. Wang, R. Z. & Weiner, S. Strain-structure relations in human teeth using Moire fringes. *J. Biomech.* **31,** 135–141 (1998).
20. Fong, H., Sarikaya, M., White, S. N. & Snead, M. L. Nano-mechanical properties profiles across dentin-enamel junction of human incisor teeth. *Mater. Sci. Eng. C* **7,** 119–128 (2000).
21. Sun, E. Y. *et al.* Debonding behavior between β-Si_3N_4 whiskers and oxynitride glasses with or without β-SiAlON interfacial layer. *Acta Mater.* **47,** 2777–2785 (1999).
22. He, M.-Y. & Hutchinson, J. W. Crack deflection at an interface between dissimilar elastic materials. *Int. J. Solids Struct.* **25,** 1053–1067 (1989).
23. Shang, J. K. & Ritchie, R. O. Crack bridging by uncracked ligaments during fatigue-crack growth in SiC-reinforced aluminum-alloy composites. *Metall. Trans. A* **20,** 897–908 (1989).
24. Kruzic, J. J., Nalla, R. K., Kinney, J. H. & Ritchie, R. O. Crack blunting, crack bridging and resistance-curve fracture mechanics of dentin: Effect of hydration. *Biomater.* **24,** 5209–5221 (2003).
25. Nalla, R. K., Kruzic, J. J., Kinney, J. H. & Ritchie, R. O. Mechanistic aspects of fracture and R-curve behavior in human cortical bone. *Biomater.* **26,** 217–231 (2005).
26. Yeni, Y. N. & Fyhrie, D. P. A rate-dependent microcrack-bridging model that can explain the strain rate dependency of cortical bone apparent yield strength. *J. Biomech.* **36,** 1343–1353 (2003).
27. Habelitz, S., Marshall ,G. W., Balloch, M. & Marshall, S. J. Nanoindentation and storage of teeth. *J. Biomechanics* **35,** 995–998 (2002).
28. Lawn, B. R. *Fracture of Brittle Solids* 2nd edn (Cambridge Univ. Press, Cambridge, 1993).
29. Dundurs, J. Edge-bonded dissimilar orthogonal elastic wedges. *J. Appl. Mech.* **36,** 650–652 (1969).
30. Ritchie, R. O. Mechanisms of fatigue crack propagation in metals, ceramics and composites: Role of crack-tip shielding. *Mater. Sci. Eng.* **103,** 15–28 (1988).

Acknowledgements

This work was supported in part by the National Institutes of Health, National Institute of Dental and Craniofacial Research, under Grant No. R01 DE 13029 (for V.I., G.W.M., S.J.M.), and by the Director, Office of Science, Office of Basic Energy Science, Division of Materials Sciences and Engineering of the Department of Energy under Contract No. DE-Ac03-76SF00098 (for J.J.K., R.O.R.). The authors wish to thank Grace Nonomura for specimen preparation, and Cynthia Chao, Kevin Liu, Earnst Young, Ravi Nalla and Eduardo Saiz for experimental assistance.

Correspondence and requests for materials should be addressed to R.O.R.

Competing financial interests

The authors declare that they have no competing financial interests.